AFF3 regulates ferroptosis and malignant progression in bladder cancer cells *via* the NRF2/GPX4 signaling axis

Song Chen, Xiangyun Li, Peiqin Zhan, Tianjiao Luo, Jiansong Wang

Department of Urology, The Second Affiliated Hospital of Kunming Medical University, Kunming, China

ABSTRACT

Bladder cancer (BCa) is a common malignancy of the urinary system, and its malignant progression is closely associated with ferroptosis. As a transcriptional regulator in the AFF family, AFF3 participates in the regulation of gene expression in multiple diseases; however, its role in BCa and its relationship with ferroptosis remain unclear. This study aimed to investigate the role of AFF3 in BCa progression and the molecular mechanism through which it regulates ferroptosis. AFF3 expression was examined through bioinformatics analysis and experiments in clinical tissues and cells. AFF3 was overexpressed in UM-UC-3 cells, and cell proliferation and migration were assessed using CCK-8, colony formation, and Transwell assays. Ferroptosis was evaluated using BODIPY 581/591 C11, MDA, and ferroptosis-related protein assays, and rescue experiments were performed with the ferroptosis inhibitor Fer-1. A subcutaneous xenograft model was established in nude mice, and the NRF2 activator TBHQ was used to verify the *in vivo* role and mechanism of AFF3 in regulating ferroptosis. Our results revealed that AFF3 was expressed at low levels in BCa. Functionally, AFF3 overexpression inhibited BCa cell proliferation, colony formation, and migration; promoted the accumulation of lipid ROS and MDA; downregulated GPX4 and SLC7A11 expression; and increased sensitivity to ferroptosis. Notably, Fer-1 partially reversed these effects. Mechanistically, AFF3 upregulated KEAP1 and inhibited NRF2 nuclear translocation, thereby reducing GPX4 expression; conversely, TBHQ partially reversed these molecular and functional changes. *In vivo* animal experiments further confirmed that AFF3 overexpression inhibited xenograft growth and promoted ferroptosis-related changes, whereas TBHQ attenuated the regulatory effects of AFF3. Overall, these findings demonstrate that AFF3 exerts tumor-suppressive effects in BCa by promoting KEAP1 expression and inhibiting NRF2 nuclear translocation and GPX4-mediated antioxidant defense, thereby enhancing the sensitivity of tumor cells to ferroptosis and suppressing the malignant progression of BCa.

Key words: bladder cancer; ferroptosis; AFF3; NRF2; GPX4.

Correspondence: Jiansong Wang, MD., Department of Urology, The Second Affiliated Hospital of Kunming Medical University, No. 374, Dianmian Avenue, Wuhua District, Kunming 650000, China.
E-mail: wangjiansong@kmmu.edu.cn

Contributions: Song Chen, conceptualization, methodology, investigation, writing – original draft, writing – review & editing. Jiansong Wang, conceptualization, methodology, investigation, writing – original draft, writing – review & editing. Xiangyun Li, data curation, formal analysis, writing – review & editing. Peiqin Zhan, data curation, formal analysis, writing – review & editing. Tianjiao Luo, formal analysis, writing – review & editing. All authors read and approved the final manuscript.

Conflict of interests: the authors declare no competing interest and all authors confirm accuracy.

Ethics approval: the study involving human bladder cancer tissues was reviewed and approved by the Ethics Committee of the Second Affiliated Hospital of Kunming Medical University (Approval No. PJ-KY-2026-211). All procedures involving human participants were conducted in accordance with the ethical principles of the Declaration of Helsinki and relevant institutional guidelines. Written informed consent was obtained from all participants before tissue collection and the use of their clinical information for research purposes. All animal experiments were reviewed and approved by the Institutional Animal Care and Use Committee of the Yunnan Besitel Biotechnology LLC (Approval No. BST-PZ-MICE-20260307-01). The animal procedures were performed in accordance with applicable institutional guidelines and national regulations for the care and use of laboratory animals. All efforts were made to minimize animal suffering and reduce the number of animals used.

Data availability statement: the datasets used and analyzed during the current study are available from the corresponding author upon reasonable request.

Introduction

Bladder cancer (BCa) is among the most common malignancies of the urinary system and is the ninth most common cancer worldwide. According to GLOBOCAN 2022 data released by the International Agency for Research on Cancer, approximately 614,000 new cases of BCa and 221,000 deaths occur worldwide each year, with men at substantially higher risk than women.[1] BCa also shows marked geographic and population differences. Although its incidence is declining, the disease burden it causes persists. Current treatments for BCa include mainly surgery, chemotherapy, immunotherapy, and targeted therapy; however, because of the high heterogeneity of BCa and treatment resistance, the clinical benefit remains very limited.[2] Therefore, an in-depth understanding of the key molecular mechanisms underlying BCa progression and the identification of new therapeutic targets are important for improving patient prognosis. Ferroptosis is an iron-dependent form of programmed cell death driven by lipid peroxidation. It is distinct from apoptosis, necrosis, and autophagy and has unique morphologic and biochemical features.[3] Numerous studies have investigated the relationship between ferroptosis and BCa and have suggested that combining conventional therapeutic agents with ferroptosis-related treatment strategies may represent a promising new approach for treating BCa.[4] However, the upstream regulatory mechanisms of ferroptosis in BCa cells have not been fully elucidated.

AF4/FMR2 family member 3 (AFF3) belongs to the AF4/FMR2 (AFF) family of transcriptional regulatory proteins, and the protein it encodes participates in the regulation of RNA polymerase II-mediated transcriptional elongation.[5] Studies have shown that AFF3 plays critical roles in the development of multiple cancers. For example, in infant patients with B-cell acute lymphoblastic leukemia, MLL (KMT2A) gene rearrangements can occur, resulting in the formation of the MLL-AFF3 fusion gene, which is associated with disease progression and poor prognosis.[6] In breast cancer, AFF3 activates an estrogen receptor-related transcriptional program to maintain tamoxifen resistance in tumor cells.[7] In addition, in castration-resistant prostate cancer, AFF3 can affect fatty acid metabolism and the ferroptosis pathway by regulating ACSL4 expression, thereby altering the sensitivity of tumor cells to the ferroptosis inducer RSL3.[8] These studies suggest that AFF3 may participate in the regulation of tumor cell metabolism and ferroptosis. Furthermore, the bioinformatics analysis performed in this study revealed that AFF3 is expressed at low levels in BCa tissues. However, the specific role of AFF3 in BCa and whether it participates in the regulation of ferroptosis require further verification.

Nuclear factor erythroid 2-related factor 2 (NRF2) is a key regulator of cellular redox homeostasis, and its activity is negatively regulated by KEAP1. Under homeostatic conditions, KEAP1 promotes the ubiquitination and degradation of NRF2; however, when cells undergo oxidative stress, NRF2 can escape KEAP1-mediated degradation and translocate to the nucleus to activate the transcription of downstream antioxidant genes.[9] Activation of NRF2 provides cytoprotection across multiple pathological states, including autoimmune diseases, neurodegenerative diseases, chronic lung and liver diseases, and cancer initiation.[10] In BCa, blocking KEAP1-mediated NRF2 degradation has been shown to increase the antioxidant capacity of tumor cells and promote cell proliferation and resistance to ferroptosis, thereby driving tumor progression.[11] In addition, GPX4 is an important effector through which NRF2 suppresses lipid peroxidation and ferroptosis. Studies have shown that GPX4 is a direct target gene of NRF2, which, upon nuclear translocation, binds to the GPX4 promoter region and initiates its transcription, thereby upregulating GPX4 expression to maintain redox balance and inhibit ferroptosis.[12] Therefore, the KEAP1-NRF2/GPX4 axis may be a key pathway regulating ferroptosis in BCa. However, a link between AFF3 and the KEAP1-NRF2/GPX4 signaling axis has not yet been established, and whether AFF3 affects ferroptosis in BCa cells and disease progression by regulating this signaling axis remains unclear. Accordingly, this study combined bioinformatics analysis, *in vitro* cell experiments, and a nude mouse xenograft model to systematically investigate the role of AFF3 in the regulation of ferroptosis in BCa and to further clarify the involvement of the KEAP1-NRF2/GPX4 signaling axis, with the aim of providing a new theoretical basis and potential targets for ferroptosis-targeted therapy in BCa.

Materials and Methods

Bioinformatics analysis

The GSE13507 microarray dataset and the TCGA-BLCA RNA-sequencing dataset were downloaded. GSE13507 contained 188 BCa tissue samples and 68 normal bladder mucosa samples, whereas TCGA-BLCA contained 411 BCa tissue samples and 19 normal bladder tissue samples. AFF3 gene expression data were subsequently extracted from all the samples, and box plots were generated using the ggplot2 package in R to compare AFF3 expression between BCa and normal bladder tissues.

Clinical sample collection

A total of 16 pairs of human BCa tissues and adjacent normal tissues were collected from patients treated at our hospital. The adjacent normal tissues were obtained more than 5 cm from the tumor margin and were pathologically confirmed to be normal bladder mucosa without tumor infiltration. After excision, the samples were fixed in 4% paraformaldehyde, dehydrated, and processed into paraffin sections for subsequent experimental analyses. Pathologists reviewed and confirmed all the cases according to the WHO classification criteria for urothelial tumors. Clinical data, including patient age, pathological grade, and TNM stage, were recorded, and long-term postoperative follow-up was conducted.

Cell culture

The normal urothelial cell line SV-HUC-1 (TCHu169) and the human BCa cell lines 5637 (TCHu 1), T24 (TCHu 55), and UM-UC-3 (TCHu217) were purchased from the Cell Bank of the Committee on Type Culture Collection of the Chinese Academy of Sciences. The cells were cultured in their respective complete culture media (MD12, MD04, MD02, and MD335) in an incubator at 37°C with 5% CO_2.

Cell treatment

To investigate the effects of AFF3 on the malignant phenotype and ferroptosis of BCa cells, UM-UC-3 cells were transduced with an AFF3-overexpressing lentivirus (OE-AFF3; 1×10^8 TU/mL; MOI = 50; GenePharma, Suzhou, China), with empty-vector lentivirus (OE-NC) used as the control. Transduction efficiency was verified by RT–qPCR and Western blotting. In addition, after stably transduced OE-AFF3 cells were plated and allowed to adhere, they were treated for 24 h with the ferroptosis inhibitor Fer-1 at a final concentration of 1 μM[13] (HY-100579; MedChemExpress, Monmouth Junction, NJ, USA). Furthermore,

OPEN ACCESS

to determine whether AFF3 regulates ferroptosis and the malignant phenotype of BCa cells through the KEAP1-NRF2/GPX4 signaling axis, stably transduced OE-AFF3 cells were plated, allowed to adhere, and then treated for 24 h with the NRF2 activator TBHQ at a final concentration of 10 μM[14] (HY-100489; MedChemExpress) for rescue experiments.

RT-qPCR

Total RNA was extracted from SV-HUC-1, T24, UM-UC-3, and 5637 cells using an RNA isolation kit (AM1912; Invitrogen, Carlsbad, CA, USA), and cDNA was synthesized using a reverse transcription kit (K1691; Invitrogen). qPCR was then performed using fluorescent qPCR premix (K0223; Invitrogen), primers, and cDNA. β-actin served as the reference gene, and relative target gene mRNA expression was calculated using the $2^{-\Delta\Delta Ct}$ method. The primer sequences are listed in Table 1.

Western blot

Total protein was extracted from SV-HUC-1, T24, UM-UC-3, and 5637 cells using RIPA lysis buffer (R0010; Solarbio, Beijing, China) supplemented with a protease/phosphatase inhibitor cocktail (P1045; Beyotime, Shanghai, China), and protein concentrations were determined using a BCA kit (P0012; Beyotime). After the samples were denatured by boiling, the proteins were separated by SDS-PAGE and transferred to PVDF membranes (88518, Thermo-Fisher Scientific, Waltham, MA, USA). The membranes were then blocked with 5% BSA (ST023; Beyotime) for 1 h at room temperature and incubated overnight at 4°C with the following primary antibodies: anti-AFF3 (1:1000; ABIN2778345; Antibodies Online, Aachen, Germany), anti-GPX4 (1:1000; 30388-1-AP; Proteintech, Rosemont, IL, USA), anti-SLC7A11 (1:4000; 32384-1-AP; Proteintech), anti-KEAP1 (1:2000; 10503-2-AP; Proteintech), anti-NRF2 (1:1000; 33123-1-AP; Proteintech, Rosemont, IL, USA), and anti-β-actin (1:5000; 20536-1-AP; Proteintech). The next day, after being washed with TBST, the membranes were incubated with secondary antibody (1:3000; S0001; Affinity, Nanjing, China) for 1 h at room temperature. Finally, the membranes were developed using ECL reagent (PE0010; Solarbio), and band intensities were quantified using ImageJ software.

CCK-8 assay

Cell viability was measured using a CCK-8 kit (HY-K0301; MedChemExpress). After UM-UC-3 cells were treated according to the experimental design, 5×10^3 cells in 100 μL were seeded per well in a 96-well plate. At 0 h, 24 h, 48 h, and 72 h after seeding, 10 μL of CCK-8 solution was added to each well. After a 2-h incubation, the absorbance at 450 nm was measured using a microplate reader. Each group included 3 replicate wells.

Colony formation assay

UM-UC-3 cells from each treatment group were trypsinized using trypsin (C0201; Beyotime) to prepare single-cell suspensions and then seeded in 6-well plates at a density of 1×10^3 cells/well. The cells were cultured for 14 d, after which the medium was replaced regularly. Once visible colonies had formed, the medium was removed, and the cells were washed with PBS and fixed in 4% paraformaldehyde (P0099; Beyotime) for 15 min at room temperature. After fixation, the cells were washed with PBS and stained with 0.1% crystal violet (G1014; Servicebio, Beijing, China) for 20 min at room temperature. The cells were then rinsed with distilled water and air-dried, and the colonies were examined under a microscope and counted.

Transwell assay

Cell migration was assessed using Transwell chambers (FTW010; Beyotime). UM-UC-3 cells in the logarithmic growth phase were washed and resuspended in serum-free medium and then counted. Next, 100 μL of cell suspension containing 2×10^4 cells was added to the upper Transwell chamber, and 600 μL of complete medium containing 10% FBS was added to the lower chamber. The cells were then cultured in an incubator for 48 h. The chambers were removed, and the cells on the inner surface of the membrane were wiped away with a sterile cotton swab. The remaining cells were fixed with absolute ethanol for 5 min and then stained with 0.1% crystal violet (G1014; Servicebio) for 5 min. After being rinsed under running water and air-dried, the cells were photographed under a microscope and counted to evaluate cell migration.

Lipid peroxidation assay

Lipid peroxidation in UM-UC-3 cells was measured using a BODIPY 581/591 C11 fluorescent probe (HY-D1301; MedChemExpress). BODIPY 581/591 C11 was dissolved in DMSO to prepare a 10 mM stock solution, which was stored at -20°C in the dark. Immediately before use, the stock solution was diluted in serum-free cell culture medium to prepare a 10 μM working solution. Single-cell suspensions of UM-UC-3 cells were prepared, washed with PBS, and incubated with BODIPY 581/591 C11 working solution for 30 min at room temperature. After incubation, the cells were centrifuged at 400 × g for 4 min at 4°C, and the supernatant was discarded. The cells were then washed with PBS, resuspended, and analyzed by fluorescence microscopy.

Immunofluorescence

UM-UC-3 cells were fixed with 4% paraformaldehyde solution (P0099; Beyotime) for 15 min at room temperature. The cells were then sequentially permeabilized with 0.3% Triton X-100 (P0096; Beyotime) for 10 min and blocked with 5% BSA (ST023; Beyotime) for 1 h at room temperature, followed by overnight incubation at 4°C with an NRF2 antibody (1:400; 33123-1-AP; Proteintech). The next day, the cells were incubated with a fluorescent secondary antibody (1:1000; ab150078; Abcam, Cambridge, UK) for 1 h in the dark. After nuclear staining with DAPI (C1006; Beyotime), NRF2 nuclear translocation was observed using a fluorescence microscope.

Subcutaneous xenograft experiments in nude mice

Male BALB/c nude mice aged 4-6 weeks (15-22 g) were purchased from the Laboratory Animal Center of Kunming Medical University and housed in cages under specific pathogen-free conditions. UM-UC-3 cells stably transduced with OE-NC or OE-AFF3 and generated as described above were collected, and 3×10^6 cells were resuspended in 100 μL of an equal-volume mixture of HBSS (HY-K3031; MedChemExpress) and Matrigel (C0371; Beyotime). The cell suspension was injected subcutaneously into the right flank of each nude mouse to establish a subcutaneous

Table 1. Primer sequences.

Gene name	Primer sequence
AFF3 (human)	F: 5′−ATTACGGAGGAAAGAACGAG-3′ R: 5′−CTTGTTAGTCTTGTAGGGCTC-3′
β-actin (human)	F: 5′−CATGTACGTTGCTATCCAGGC-3′ R: 5′−CTCCTTAATGTCACGCACGAT-3′

xenograft model.[15,16] The tumor-bearing mice were randomly assigned to one of 3 groups: OE-NC, OE-AFF3, or OE-AFF3+TBHQ. Mice in the OE-AFF3+TBHQ group received daily intraperitoneal injections of the NRF2 activator TBHQ at 20 mg/kg[17] (HY-100489; MedChemExpress) for 28 d, whereas mice in the other two groups received an equal volume of normal saline as the control. Body weight and tumor volume were measured every 7 d. At the experimental endpoint, the mice were euthanized, and the xenografts were excised and weighed for subsequent analyses.

Immunohistochemistry

Clinical BCa tissues and subcutaneous xenografts from nude mice were collected, fixed in 4% paraformaldehyde, dehydrated through a graded ethanol series, embedded in paraffin, and sectioned. The sections were deparaffinized and rehydrated, and antigen retrieval was performed in sodium citrate antigen retrieval solution (P0081; Beyotime) in a 95°C water bath for 20 min. After cooling to room temperature, endogenous peroxidase activity was blocked for 10 min at room temperature with endogenous peroxidase blocking solution (E752115; Aladdin, Shanghai, China), and nonspecific binding was blocked for 30 min at room temperature with 5% goat serum (SL038; Solarbio). The sections were then incubated separately overnight at 4°C in a humidified chamber with the following primary antibodies: anti-AFF3 (1:500; ab106231; Abcam), anti-Ki67 (1:8000; 27309-1-AP; Proteintech), anti-NRF2 (1:200; 16396-1-AP; Proteintech), and anti-GPX4 (1:500; 30388-1-AP; Proteintech). The following day, the sections were incubated with secondary antibody (1:200; S0001; Affinity) for 1 h at room temperature, developed with DAB (DA1010; Solarbio), counterstained to visualize the nuclei, dehydrated, cleared, mounted, and examined microscopically.

Malondialdehyde (MDA) assay

An MDA content assay kit (BC0025; Solarbio) was used. An appropriate amount of subcutaneous xenograft tissue from nude mice was homogenized on ice in extraction buffer and centrifuged at 8000× g for 10 min at 4°C; the supernatant was collected as the test sample. UM-UC-3 cells were sonicated in extraction buffer and centrifuged under the same conditions, after which the supernatant was collected for testing. The samples were loaded according to the kit instructions, and the absorbance of each group was measured at the corresponding wavelength using a microplate reader to calculate the MDA level in each group.

Statistical analysis

Data were analyzed using GraphPad Prism 8.0 (La Jolla, CA, USA) and are expressed as the mean ±SD. The Shapiro-Wilk test was performed to verify the normal distribution of the data. Comparisons between two groups were carried out using an independent-samples *t*-test, and one-way or two-way analysis of variance (ANOVA) followed by Tukey's *post-hoc* test was used for multiple-group pairwise comparisons. A p value of less than 0.05 was considered to indicate statistical significance.

Results

AFF3 is downregulated in BCa

To identify key pathogenic molecules in BCa, we performed bioinformatics analyses using the TCGA-BLCA and GSE13507 datasets. The results revealed that AFF3 expression was significantly lower in BCa tissues than in normal bladder tissues (Figure 1A). To validate the bioinformatics findings, we collected BCa tissues (tumor group) and paired adjacent normal tissue samples (normal group) for clinical validation. Immunohistochemical staining revealed that AFF3 expression was significantly lower in the tumor group than in the normal group (Figure 1B). Together, these results demonstrate that AFF3 is downregulated in BCa, suggesting that it may be involved in BCa progression.

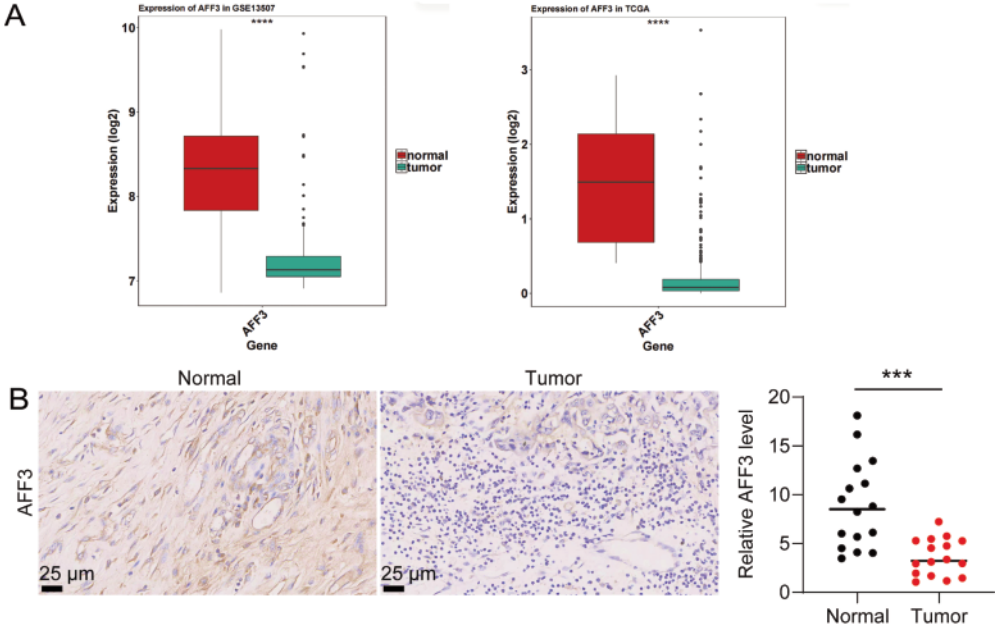


Figure 1. AFF3 is downregulated in BCa. **A**) Bioinformatics analysis of differences in AFF3 expression between BCa and normal bladder tissues. **B**) Immunohistochemical analysis of AFF3 protein expression in clinical tumor and adjacent normal tissues; scale bar: 25 μm. ***p<0.001 *vs* normal group.

OPEN ACCESS

AFF3 overexpression inhibits BCa cell proliferation and migration

To define the role of AFF3 in BCa progression, we performed further *in vitro* validation. We first measured AFF3 expression in normal bladder urothelial SV-HUC-1 cells and three BCa cell lines (T24, 5637, and UM-UC-3). Both AFF3 mRNA and protein levels were significantly lower in all three BCa cell lines than in SV-HUC-1 cells, with the greatest reduction observed in UM-UC-3 cells (Figure 2 A,B); therefore, this cell line was selected for subsequent functional assays and mechanistic validation. UM-UC-3 cells were transduced with a lentiviral vector to establish a stable AFF3-overexpressing (OE-AFF3) cell line, and the transduction efficiency was confirmed by RT-qPCR and Western blotting

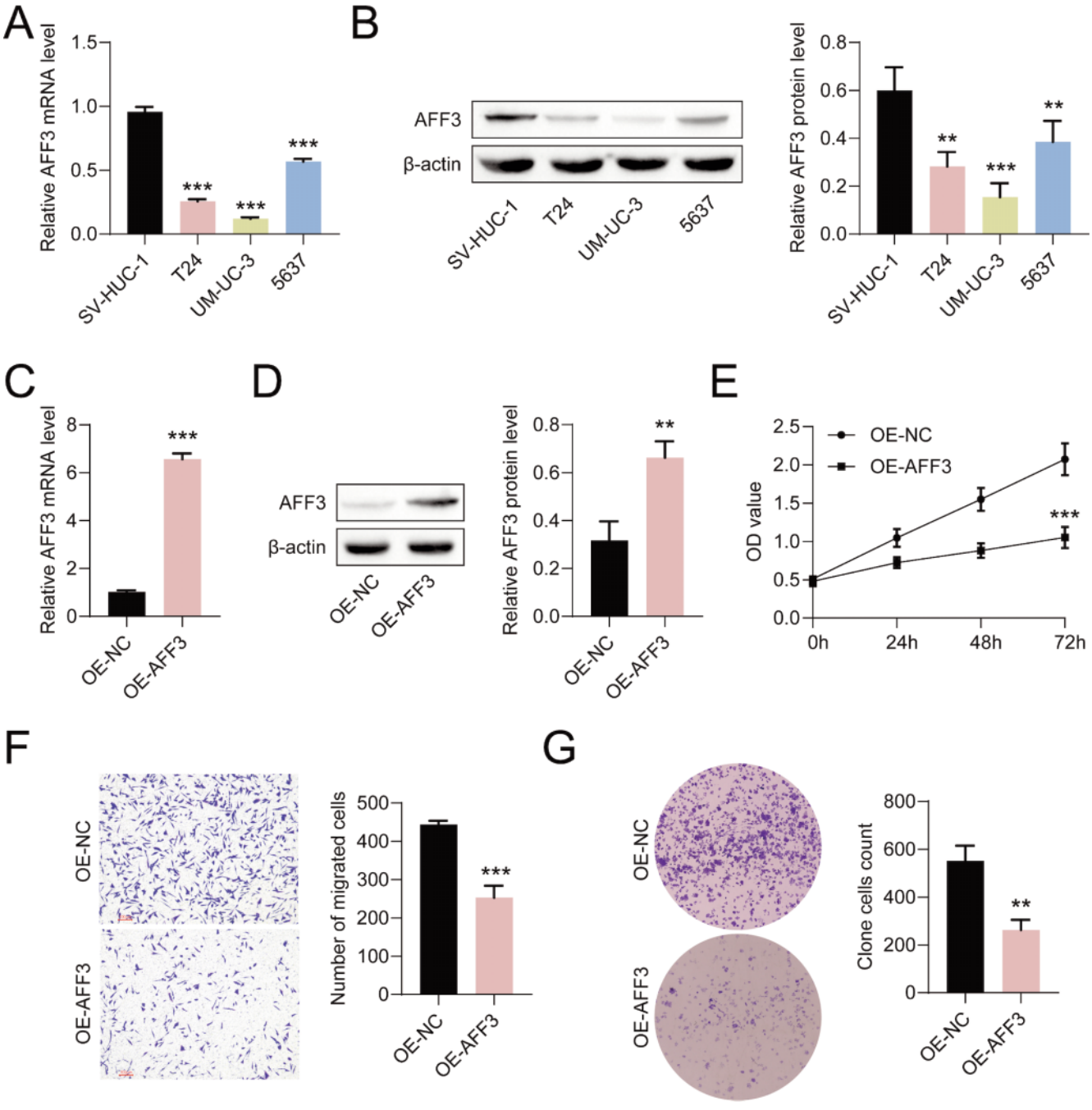


Figure 2. AFF3 overexpression inhibits BCa cell proliferation and migration. **A**) RT-qPCR analysis of AFF3 expression in normal urothelial cells and BCa cells. **B**) Western blot analysis of AFF3 expression in normal urothelial cells and BCa cells. **C**) RT-qPCR confirmation of AFF3 overexpression in UM-UC-3 cells. **D**) Western blot confirmation of AFF3 overexpression in UM-UC-3 cells. **E**) CCK-8 assay of cell viability. **F**) Transwell migration assay; scale bar: 100 μm. **G**) Colony formation assay of cell proliferation. $^{**}p<0.01$, $^{***}p<0.001$ *vs* SV-HUC-1 group and OE-NC group.

(Figure 2 C,D). The results of the CCK-8 assay revealed that UM-UC-3 cell viability was significantly lower in the OE-AFF3 group than in the OE-NC group (Figure 2E). Transwell assays revealed significantly fewer cells in the AFF3-overexpressing group than in the OE-NC group, indicating impaired migration (Figure 2F). The results of the colony formation assay further revealed that AFF3 overexpression markedly reduced the number of colonies formed (Figure 2G), indicating suppressed cell proliferation. Collectively, these findings demonstrate that AFF3 overexpression significantly suppresses the proliferative and migratory malignant phenotypes of BCa cells.

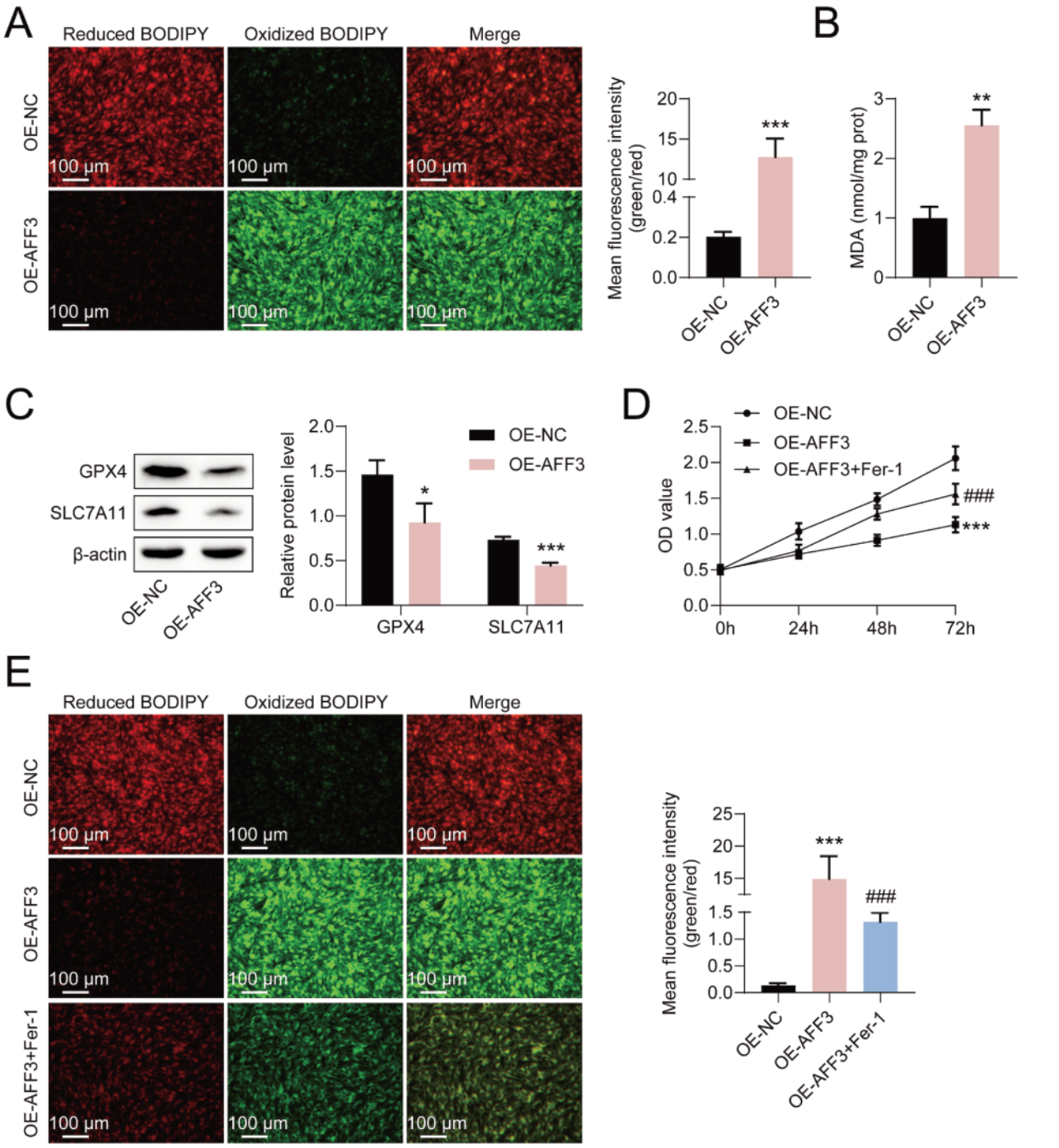


Figure 3. AFF3 overexpression promotes lipid peroxidation and induces ferroptosis in BCa cells. **A**) BODIPY 581/591 C11 staining to assess lipid ROS levels; scale bar: 100 μm. **B**) Measurement of the MDA content using an assay kit. **C**) Western blot analysis of the ferroptosis-related proteins GPX4 and SLC7A11. **D**) CCK-8 assay of cell viability. **E**) BODIPY 581/591 C11 staining to assess the reversal of lipid ROS accumulation by Fer-1. *p<0.05, **p<0.01, ***p<0.001 *vs* the OE-NC group; $^{###}p$<0.001 *vs* OE-AFF3 group.

OPEN ACCESS

AFF3 overexpression promotes lipid peroxidation and induces ferroptosis in BCa cells

To determine whether the suppression of malignant BCa cell phenotypes by AFF3 was associated with the ferroptosis pathway, we first examined ferroptosis-related markers. BODIPY 581/591 C11 staining revealed markedly higher cellular lipid ROS levels in the OE-AFF3 group than in the OE-NC group (Figure 3A). The results of the MDA assay confirmed that AFF3 overexpression significantly increased the intracellular levels of MDA, an end product of lipid peroxidation (Figure 3B). AFF3 overexpression also markedly reduced the expression of the ferroptosis-suppressing proteins GPX4 and SLC7A11 (Figure 3C). To further determine whether AFF3-mediated cell injury was induced by ferroptosis, we performed rescue experiments with the ferroptosis inhibitor Fer-1 in AFF3-overexpressing cells. Fer-1 markedly reversed the decrease in cell viability caused by AFF3 overexpression (Figure 3D) and alleviated AFF3-induced lipid ROS accumulation (Figure 3E). These results indicate that AFF3 overexpression promotes lipid peroxidation and induces ferroptosis in BCa cells.

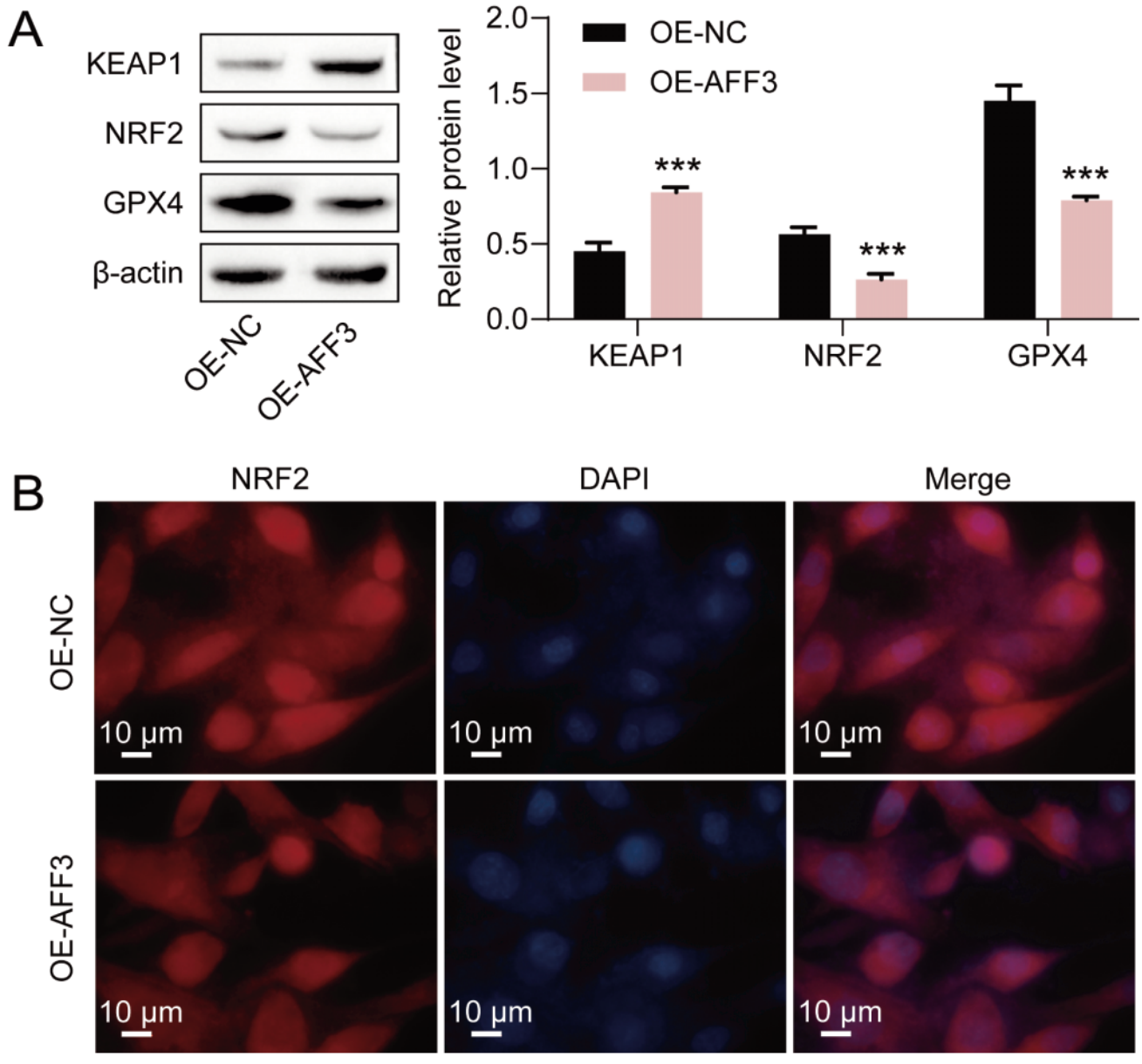


Figure 4. AFF3 regulates the KEAP1-NRF2/GPX4 signaling axis. **A**) Western blot analysis of the effects of AFF3 overexpression on KEAP1, NRF2, and GPX4 protein expression. **B**) Immunofluorescence analysis of changes in NRF2 subcellular localization. ***p<0.001 vs OE-NC group.

AFF3 regulates the KEAP1-NRF2/GPX4 signaling axis

To further investigate the potential molecular mechanism through which AFF3 induces ferroptosis in BCa cells, we examined changes in key components of the KEAP1-NRF2/GPX4 signaling axis, given its critical role in ferroptosis regulation. Compared with those in the OE-NC group, the expression of KEAP1 in the OE-AFF3 group significantly increased, whereas the expression of NRF2 and downstream GPX4 significantly decreased (Figure 4A). Immunofluorescence staining revealed markedly reduced nuclear NRF2 fluorescence following AFF3 overexpression, with NRF2 localized predominantly to the cytoplasm (Figure 4B), indicating impaired NRF2 nuclear translocation. These findings indicate that AFF3 upregulates KEAP1 expression, thereby suppressing NRF2 activation and nuclear translocation and reducing GPX4 expression.

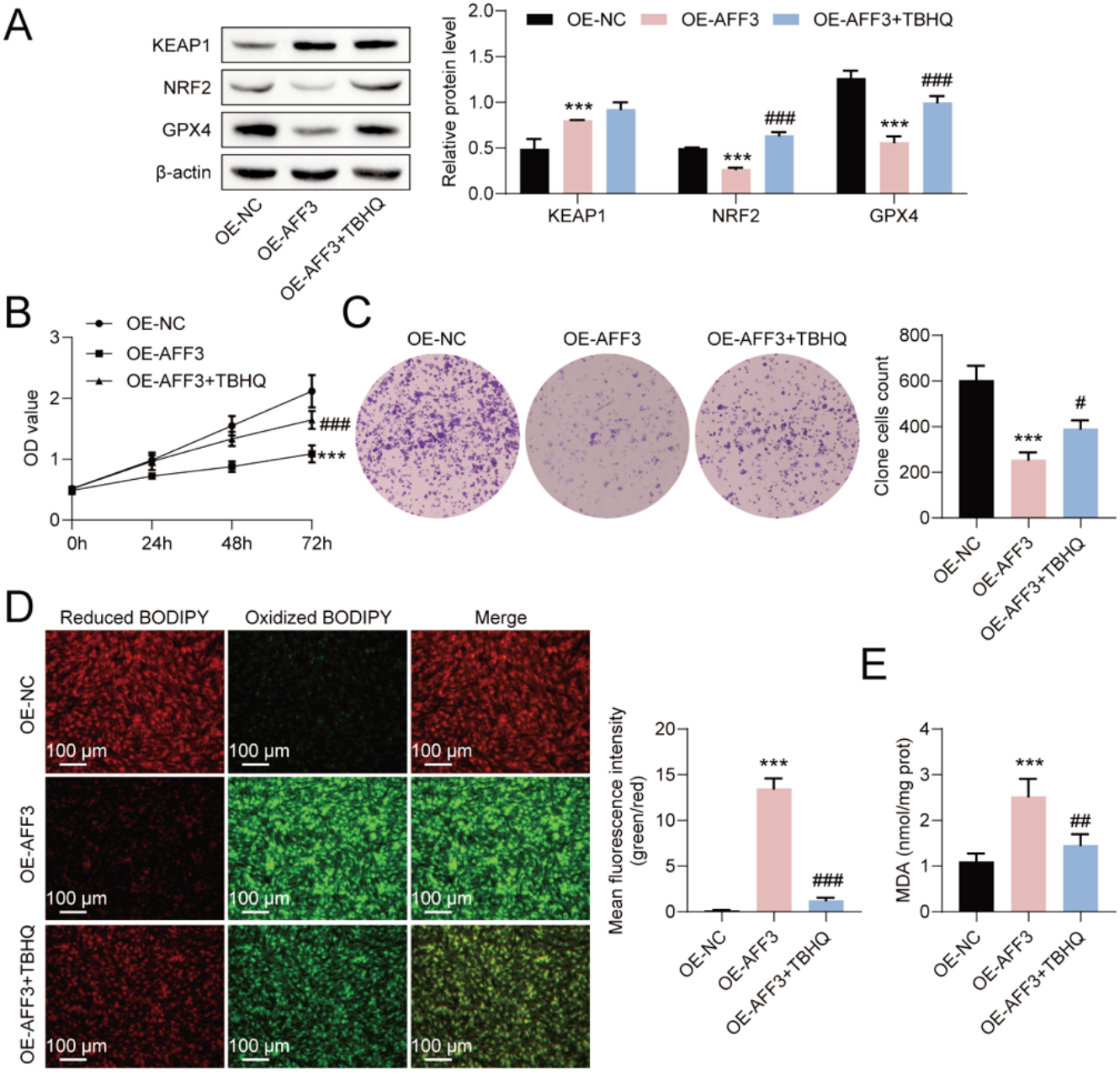


Figure 5. AFF3 regulates ferroptosis and malignant phenotypes in BCa cells via the KEAP1-NRF2/GPX4 signaling axis. **A**) Western blot analysis of the effects of TBHQ on KEAP1, NRF2, and GPX4 protein expression in AFF3-overexpressing cells. **B**) CCK-8 assay of cell viability. **C**) Colony formation assay of proliferation. **D**) BODIPY 581/591 C11 staining to assess lipid ROS levels. E) Measurement of the MDA content using an assay kit. ***$p<0.001$ *vs* the OE-NC group; $^{\#}p<0.05$, $^{\#\#}p<0.01$, $^{\#\#\#}p<0.001$ *vs* OE-AFF3 group.

OPEN ACCESS

AFF3 regulates ferroptosis and malignant phenotypes in BCa cells *via* the KEAP1−NRF2/GPX4 signaling axis

To determine whether AFF3 regulates ferroptosis and malignant phenotypes in BCa cells through the KEAP1-NRF2/GPX4 signaling axis, we performed rescue experiments with the NRF2 activator TBHQ in AFF3-overexpressing cells. TBHQ treatment reversed the AFF3 overexpression-induced decreases in NRF2 and GPX4 expression but did not significantly affect KEAP1 levels (Figure 5A), further supporting that KEAP1 acts upstream of NRF2/GPX4 in this signaling cascade. TBHQ partially reversed the AFF3 overexpression-induced reductions in cell viability and colony-forming capacity, as indicated by the CCK-8 and colony formation assays, respectively (Figure 5 B,C). In addition, TBHQ markedly reduced AFF3-induced lipid ROS accumulation (Figure 5D) and decreased the intracellular MDA content (Figure 5E).

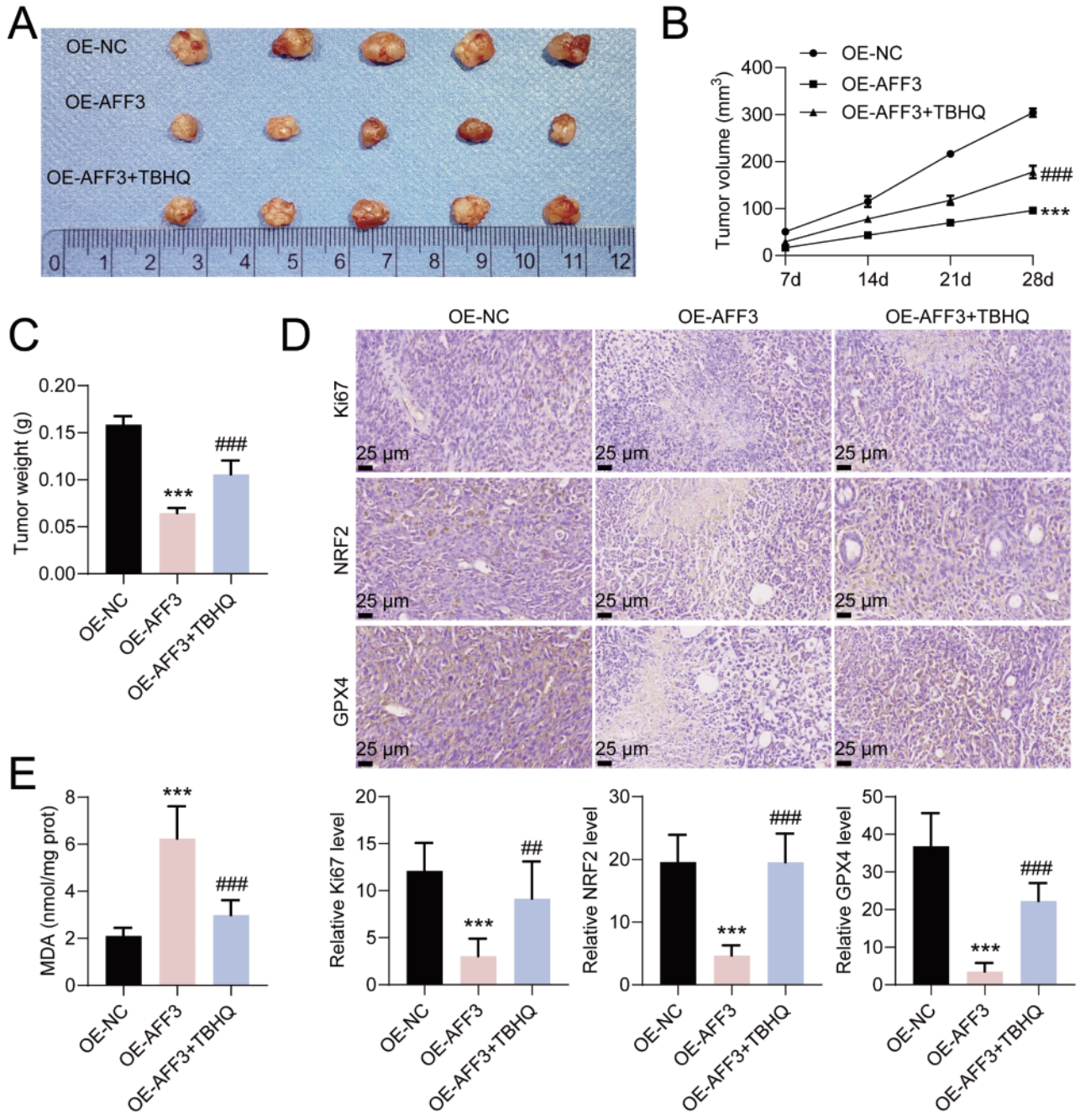


Figure 6. AFF3 suppresses tumor growth and induces ferroptosis in vivo by inhibiting the NRF2/GPX4 signaling axis. **A**) Gross images of nude mouse tumors. **B**) Changes in tumor volume among the groups. **C**) Xenograft weights in each group. **D**) Immunohistochemical analysis of Ki67, NRF2, and GPX4 expression in tumor tissues. **E**) Measurement of the MDA content in tumor tissues. ***p<0.001 *vs* OE-NC group; ###p<0.001 *vs* OE-AFF3 group.

These results indicate that AFF3 promotes ferroptosis and inhibits proliferation in BCa cells by suppressing the KEAP1-NRF2/GPX4 signaling axis.

AFF3 suppresses tumor growth and induces ferroptosis *in vivo* by inhibiting the NRF2/GPX4 signaling axis

Finally, to validate the regulatory effects of AFF3 on tumor growth and ferroptosis *in vivo*, we established a subcutaneous xenograft model in nude mice using UM-UC-3 cells. Compared with that in the OE-NC group, the subcutaneous tumor volume increased markedly more slowly in the OE-AFF3 group, and the tumor weight at the experimental endpoint was markedly lower. TBHQ treatment attenuated these inhibitory effects, resulting in marked increases in tumor volume and weight (Figure 6 A-C). Immunohistochemical analysis revealed that Ki67 expression, as well as NRF2 and GPX4 expression, was markedly lower in the OE-AFF3 group than in the OE-NC group; after TBHQ treatment, the expression levels of Ki67, NRF2, and GPX4 increased significantly (Figure 6D). Measurements of the MDA content in tumor tissue revealed that AFF3 overexpression markedly increased MDA levels, whereas TBHQ treatment substantially reduced MDA accumulation (Figure 6E). These findings confirm that AFF3 induces lipid peroxidation and ferroptosis in tumor tissue by suppressing NRF2/GPX4 signaling, thereby inhibiting BCa tumor growth *in vivo*.

Discussion

BCa is a urologic malignancy characterized by high risks of recurrence and progression and the need for long-term disease management. BCa places a substantial burden on health care systems worldwide, and numerous challenges remain in its treatment.[18,19] This study investigated the expression patterns and biological functions of AFF3 in BCa, as well as the mechanism through which AFF3 regulates ferroptosis. Analysis of public databases and validation in clinical tissue samples confirmed that AFF3 is expressed at low levels in BCa. Further experiments revealed that AFF3 overexpression suppressed malignant phenotypes in BCa cells and promoted ferroptosis; these effects were partially reversed by Fer-1, indicating that the tumor-suppressive role of AFF3 is closely associated with ferroptosis. Mechanistic studies suggested that AFF3 may promote ferroptosis by inhibiting the KEAP1/NRF2/GPX4 signaling axis. Nude mouse xenograft experiments further confirmed the *in vivo* effects of AFF3 on BCa tumor growth and ferroptosis. Taken together, these findings suggest that low AFF3 expression may activate the KEAP1/NRF2/GPX4 signaling axis, increase antioxidant defenses, reduce the sensitivity of tumor cells to ferroptosis, and thereby promote the malignant progression of BCa.

Ferroptosis is characterized by abnormal intracellular accumulation of lipid peroxides, whereas the SLC7A11/GPX4 antioxidant system is an important defense mechanism for maintaining cellular redox homeostasis and regulating ferroptosis.[20] SLC7A11 maintains GSH synthesis by promoting cysteine uptake, whereas GPX4 uses GSH to eliminate lipid peroxides, thereby suppressing iron-dependent oxidative damage to lipids and preventing ferroptosis.[21] Studies in BCa have shown that SLC7A11 and GPX4 are aberrantly overexpressed and that their overexpression is associated with evasion of ferroptosis by tumor cells and poor patient prognosis. The inhibition of SLC7A11/GPX4 has also been shown to promote ferroptosis in BCa cells, suppress malignant phenotypes, and enhance chemosensitivity.[22-24] The present study further revealed that AFF3 overexpression downregulated SLC7A11 and GPX4 levels and increased lipid ROS and MDA levels. Fer-1 treatment reversed AFF3-induced lipid peroxide accumulation and loss of cell viability, further supporting the proferroptotic role of AFF3.

KEAP1-NRF2 signaling is a key pathway through which cells respond to oxidative stress and maintain redox homeostasis.[25] Current evidence indicates that the KEAP1-NRF2 system interacts with multiple cellular signaling and metabolic pathways, making NRF2 a key regulatory node for diverse disease phenotypes.[26] In BCa, disruption of KEAP1–NRF2 binding has been shown to inhibit ferroptosis in tumor cells.[11] Shao *et al*.[27] reported that periplogenin promoted NRF2 ubiquitination and degradation, reduced the expression of NRF2 and downstream ferroptosis-inhibitory proteins such as GPX4, and consequently increased the accumulation of iron ions and lipid peroxides and induced ferroptosis in BCa cells. The results of the present study revealed that AFF3 overexpression increased KEAP1 expression, inhibited NRF2 nuclear translocation, and reduced GPX4 levels, whereas TBHQ partially restored GPX4 expression and mitigated the AFF3 overexpression-induced loss of cell viability, inhibition of proliferation, and accumulation of lipid peroxides. These findings suggest that the KEAP1/NRF2/GPX4 signaling axis is an important downstream pathway through which AFF3 exerts its proferroptotic and antitumor effects.

AFF3 plays a key role in transcriptional elongation and was initially identified through its association with lymphoid development and leukemogenesis.[28] Aberrant AFF3 expression is closely associated with multiple diseases, particularly cancer and neurologic disorders. For example, AFF3 participates in MLL fusion protein-mediated P-TEFb recruitment and aberrant transcriptional elongation, thereby maintaining persistent leukemic transcriptional programs.[29] Expansion of GCC repeats in the AFF3 promoter region is associated with neurodevelopmental disorders and intellectual disability.[30] Recent studies of prostate cancer have also suggested that AFF3 loss is accompanied by reduced ACSL4 expression and decreased sensitivity to ferroptosis.[8] However, the function of AFF3 in BCa and its regulatory relationship with the KEAP1-NRF2/GPX4 signaling axis remain unclear. This study is the first to link AFF3 to ferroptosis regulation in BCa, suggesting that AFF3 not only participates in transcriptional regulation but also may modulate ferroptosis in solid tumors by affecting redox homeostasis, thereby broadening the scope of AFF3 research in cancer. In conclusion, the results of this study demonstrate that AFF3 upregulates KEAP1 expression and inhibits NRF2 nuclear translocation, thereby downregulating GPX4 and the antioxidant defenses it mediates, promoting lipid peroxidation and ferroptosis in BCa cells and ultimately suppressing tumor proliferation, migration, and tumorigenicity *in vivo*. These findings suggest that the AFF3/KEAP1/NRF2/GPX4 regulatory axis may represent a potential research target for ferroptosis-based intervention in BCa. However, this study has several limitations. First, all functional experiments were performed solely in the UM-UC-3 cell line, which has a unique genetic background. Further validation of our key findings in additional BCa cell lines will be needed in future work to improve the generalizability of these results. Second, the direct molecular mechanism through which AFF3 regulates KEAP1 expression remains unclear. Future studies could investigate this mechanism using RNA sequencing, chromatin immunoprecipitation, RNA stability analysis, or protein degradation experiments. Finally, the clinical sample size in this study was relatively small. The associations of AFF3 with clinical stage, pathological grade, treatment response, and patient prognosis in BCa should be evaluated in larger, multicenter, independent cohorts.

OPEN ACCESS

References

1. Filho AM, Briganti A, Jemal A, Bray F. Bladder cancer incidence and mortality: a global overview and recent trends. Eur Urol 2026;89:426-36.
2. Lopez-Beltran A, Cookson MS, Guercio BJ, Cheng L. Advances in diagnosis and treatment of bladder cancer. BMJ 2024;384:e076743.
3. Dixon SJ, Olzmann JA. The cell biology of ferroptosis. Nat Rev Mol Cell Biol 2024;25:424-42.
4. An WX, Gupta R, Zhai K, Wang YR, Xu WH, Cui Y. Current and potential roles of ferroptosis in bladder cancer. Curr Med Sci 2024;44:51-63.
5. Luo Z, Lin C, Guest E, Garrett AS, Mohaghegh N, Swanson S, et al. The super elongation complex family of RNA polymerase II elongation factors: gene target specificity and transcriptional output. Mol Cell Biol 2012;32:2608-17.
6. von Bergh ARM, Beverloo HB, Rombout P, van Wering ER, van Weel MH, Beverstock GC, et al. LAF4, an AF4-related gene, is fused to MLL in infant acute lymphoblastic leukemia. Gene Chromosome Canc 2002;35:92-6.
7. Shi Y, Zhao Y, Zhang Y, AiErken N, Shao N, Ye R, et al. AFF3 upregulation mediates tamoxifen resistance in breast cancers. J Exp Clin Canc Res 2018;37:254.
8. Fan A, Li Y, Zhang Y, Meng W, Pan W, Chen M, et al. Loss of AR-regulated AFF3 contributes to prostate cancer progression and reduces ferroptosis sensitivity by downregulating ACSL4 based on single-cell sequencing analysis. Apoptosis 2024;29:1679-95.
9. Bellezza I, Giambanco I, Minelli A, Donato R. Nrf2-Keap1 signaling in oxidative and reductive stress. Biochim Biophys Acta Mol Cell Res 2018;1865:721-33.
10. Cuadrado A, Rojo AI, Wells G, Hayes JD, Cousin SP, Rumsey WL, et al. Therapeutic targeting of the NRF2 and KEAP1 partnership in chronic diseases. Nat Rev Drug Discov 2019;18:295-317.
11. Fan L, Guo D, Zhu C, Gao C, Wang Y, Yin F, et al. LRRC45 accelerates bladder cancer development and ferroptosis inhibition via stabilizing NRF2 by competitively KEAP1 interaction. Free Radic Biol Med 2025;226:29-42.
12. Kang X, Huo Y, Jia S, He F, Li H, Zhou Q, et al. Silenced LINC01134 enhances oxaliplatin sensitivity by facilitating ferroptosis through GPX4 in hepatocarcinoma. Front Oncol 2022;12:939605.
13. Zhu H, Chen Q, Zhang Y, Zhao L. Glutathione S-transferase zeta 1 alters the HMGB1/GPX4 axis to drive ferroptosis in bladder cancer cells. Hum Exp Toxicol 2023;42:9603271231161606.
14. Xiang Y, Chen X, Wang W, Zhai L, Sun X, Feng J, et al. Natural product erianin inhibits bladder cancer cell growth by inducing ferroptosis via NRF2 inactivation. Front Pharmacol 2021;12:775506.
15. Ramakrishnan S, Huss W, Foster B, Ohm J, Wang J, Azabdaftari G, et al. Transcriptional changes associated with in vivo growth of muscle-invasive bladder cancer cell lines in nude mice. Am J Clin Exp Urol 2018;6:138-48.
16. Ru R, Chen G, Liang X, Cao X, Yuan L, Meng M. Sea cucumber derived triterpenoid glycoside frondoside A: a potential anti-bladder cancer drug. Nutrients 2023;15:378.
17. Yang X, Song W, Lu Z, Chen Y, Wang Y, Huang T, et al. Lycopene mitigates T-2 toxin-induced hepatic ferroptosis by targeting the Nrf2/mitophagy axis in mice. Npj Sci Food 2026;10:94.
18. Richters A, Aben KKH, Kiemeney LALM. The global burden of urinary bladder cancer: an update. World J Urol 2020;38:1895-904.
19. Jian N, Yu L, Ma L, Zheng B, Huang W. BCG therapy in bladder cancer and its tumor microenvironment interactions. Clin Microbiol Rev 2025;38:e0021224.
20. Rochette L, Dogon G, Rigal E, Zeller M, Cottin Y, Vergely C. Lipid peroxidation and iron metabolism: two corner stones in the homeostasis control of ferroptosis. Int J Mol Sci 2022;24:449.
21. Liu X, Chen C, Han D, Zhou W, Cui Y, Tang X, et al. SLC7A11/GPX4 inactivation-mediated ferroptosis contributes to the pathogenesis of triptolide-induced cardiotoxicity. Oxid Med Cell Longev 2022;2022:3192607.
22. Li W, Ou Y, Ye F, Cheng Z, Chen Z, Zhou Q, et al. cirSIRT5 induces ferroptosis in bladder cancer by forming a ternary complex with SYVN1/PHGDH. Cell Death Discov 2024;10:391.
23. Sun Y, Berleth N, Wu W, Schlütermann D, Deitersen J, Stuhldreier F, et al. Fin56-induced ferroptosis is supported by autophagy-mediated GPX4 degradation and functions synergistically with mTOR inhibition to kill bladder cancer cells. Cell Death Dis 2021;12:1028.
24. Zhao Y, Ren P, Yang Z, Wang L, Hu C. Inhibition of SND1 overcomes chemoresistance in bladder cancer cells by promoting ferroptosis. Oncol Rep 2023;49:16.
25. Suzuki T, Takahashi J, Yamamoto M. Molecular basis of the KEAP1-NRF2 signaling pathway. Mol Cells 2023;46:133-41.
26. Baird L, Yamamoto M. The molecular mechanisms regulating the KEAP1-NRF2 pathway. Mol Cell Biol 2020;40:e00020-99.
27. Shao YQ, Sheng DY, Guan YJ, Mi EXT, Hu CY, Lu QF, et al. [Mechanism of periplogenin in promoting Nrf2 degradation and inducing ferroptosis to inhibit bladder cancer].[Article in Chinese with English Abstract]. Zhongguo Zhong Yao Za Zhi 2025;50:5790-9.
28. Zhang Y, Liang J. Research progress on the KMT2A-AFF3 fusion gene in childhood acute lymphoblastic leukemia: mechanisms, clinical implications, and therapeutic strategies. Curr Issues Mol Biol 2025;47:988.
29. Mueller D, García-Cuéllar MP, Bach C, Buhl S, Maethner E, Slany RK. Misguided transcriptional elongation causes mixed lineage leukemia. Plos Biol 2009;7:e1000249.
30. Jadhav B, Garg P, van Vugt JJFA, Ibanez K, Gagliardi D, Lee W, et al. A phenome-wide association study of methylated GC-rich repeats identifies a GCC repeat expansion in AFF3 associated with intellectual disability. Nat Genet 2024;56:2322-32.

Received: 22 August 2026. Accepted: 16 September 2026.

This work is licensed under a Creative Commons Attribution-NonCommercial 4.0 International License (CC BY-NC 4.0).
©Copyright: the Author(s), 2026
Licensee PAGEPress, Italy
European Journal of Histochemistry 2026; 70:4756
doi:10.4081/ejh.2026.4756

Publisher's note: all claims expressed in this article are solely those of the authors and do not necessarily represent those of their affiliated organizations, or those of the publisher, the editors and the reviewers. Any product that may be evaluated in this article or claim that may be made by its manufacturer is not guaranteed or endorsed by the publisher.

OPEN ACCESS